

Optical Control of Muscle Function by Transplantation of Stem Cell–Derived Motor Neurons in Mice

J. Barney Bryson,¹ Carolina Barcellos Machado,^{2*} Martin Crossley,^{2*} Danielle Stevenson,^{2*} Virginie Bros-Facer,¹ Juan Burrone,² Linda Greensmith,^{1,3††} Ivo Lieberam^{2††}

Damage to the central nervous system caused by traumatic injury or neurological disorders can lead to permanent loss of voluntary motor function and muscle paralysis. Here, we describe an approach that circumvents central motor circuit pathology to restore specific skeletal muscle function. We generated murine embryonic stem cell–derived motor neurons that express the light-sensitive ion channel channelrhodopsin-2, which we then engrafted into partially denervated branches of the sciatic nerve of adult mice. These engrafted motor neurons not only reinnervated lower hind-limb muscles but also enabled their function to be restored in a controllable manner using optogenetic stimulation. This synthesis of regenerative medicine and optogenetics may be a successful strategy to restore muscle function after traumatic injury or disease.

Electrical stimulation of motor axons within peripheral nerves has been known to induce muscle contraction since Luigi Galvani's early experiments. In more recent times, phrenic nerve pacing has been used clinically to control

the function of the diaphragm, the major muscle involved in respiration, in some patients with high-level spinal cord injury (1) or amyotrophic lateral sclerosis (ALS) (2). However, peripheral nerves are composed of efferent motor axons as well as afferent sensory axons (which are unaffected in ALS). Functional electrical stimulation, which stimulates nerves indiscriminately, can thus cause considerable discomfort (3). Furthermore, functional electrical stimulation is ineffective if axon integrity is compromised because of injury or degenerative disease. Other strategies to replace lost motor neurons within the central nervous system include the use of embryonic stem cells (ESCs), but ESC-derived neurons do not always integrate

into adult brain and spinal cord circuitry (4) and have difficulty overcoming molecular inhibitors of neuronal outgrowth (5) and extending axons across the barrier between the central and peripheral nervous system to reach the appropriate muscles (6).

It has previously been shown that motor neurons derived from ESCs can be engrafted into a peripheral nerve environment and successfully reinnervate denervated muscle (7). However, these engrafted cells are not connected to the descending inputs within the central nervous system that normally control motor function; therefore, their neural activity must be regulated by an artificial control system. Such engrafted ESC-derived motor neurons can be electrically stimulated (7), but this approach stimulates endogenous as well as engrafted neurons. In transgenic mice that express the light-sensitive ion channel channelrhodopsin-2 (ChR2) (8, 9) in endogenous motor neurons, it has been shown that the axons of these ChR2 motor neurons can be recruited by optical stimulation in a physiological and graded fashion, resulting in optogenetic control of muscle function (10). It has also been shown that viral expression of ChR2 in motor neurons of adult rats can enable optical stimulation of muscle function (11). In this study, we tested whether expression of ChR2 in ESC-derived motor neurons engrafted into a denervated peripheral nerve (i) confers optically regulated control of muscle function, without interfering with endogenous motor signals or afferent sensory axons, and (ii) enables physiological recruitment of motor units.

We generated genetically modified ESC-derived motor neurons that express both ChR2, to enable

¹Sobell Department of Motor Neuroscience and Movement Disorders, University College London (UCL) Institute of Neurology, London, UK. ²Medical Research Council (MRC) Centre for Developmental Neurobiology, King's College London, Guy's Hospital Campus, London, UK. ³MRC Centre for Neuromuscular Diseases, UCL Institute of Neurology, London, UK.

*These authors contributed equally to this work.

†These authors contributed equally to this work.

††Corresponding author. E-mail: l.greensmith@ucl.ac.uk (L.G.); ivo.lieberam@kcl.ac.uk (I.L.)

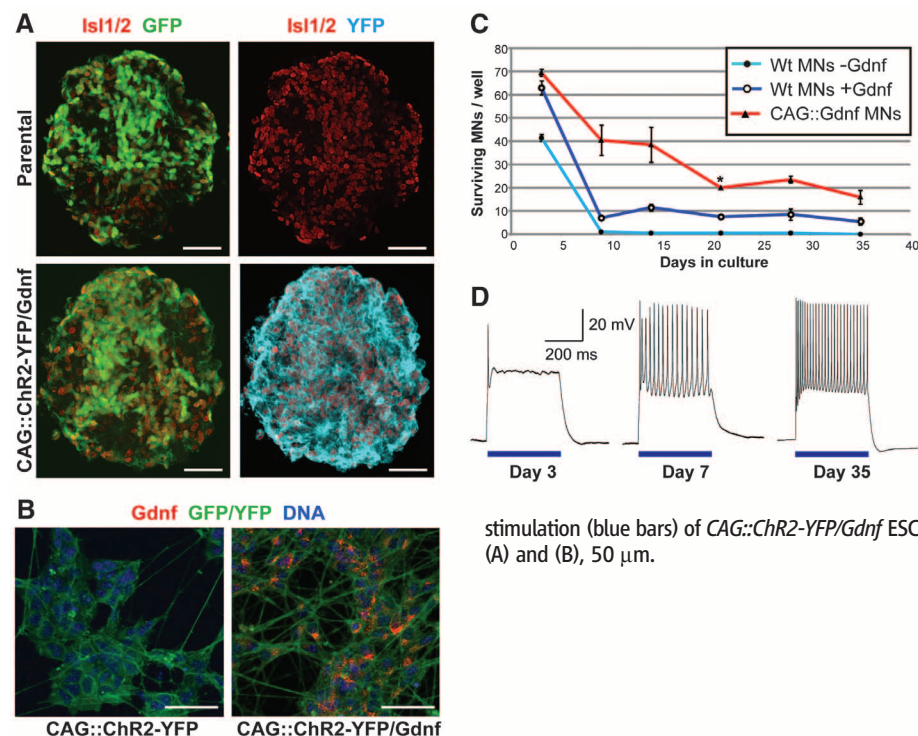


Fig. 1. Expression of Gdnf in ChR2 motor neurons enhances survival and enables them to mature electrically in vitro. (A) Embryoid bodies derived from *CAG::ChR2-YFP/Gdnf* transgenic ESCs and parental controls stained for the pan-motor neuron marker *Isl1/2*. GFP and YFP signals were detected by direct fluorescence. (B) Confocal images of MACS-sorted ESC motor neurons derived from *CAG::ChR2-YFP* (MACS, magnetic-activated cell sorting) and *CAG::ChR2-YFP/Gdnf* ESCs immunostained for Gdnf and GFP/YFP. (C) Survival analysis of sorted *CAG::ChR2-YFP* and *CAG::ChR2-YFP/Gdnf* ESC motor neurons (MNs) (200 cells per well) plated on ESC astrocytes at indicated time points. *CAG::ChR2-YFP* motor neurons were cultured with (10 ng/ml) or without recombinant Gdnf (two replicates, analysis of variance with Bonferroni correction, * $P < 0.25$). Error bars indicate SEM. One representative of three separate experiments is shown. Wt, wild type. (D) Optogenetic stimulation (blue bars) of *CAG::ChR2-YFP/Gdnf* ESC motor neurons cultured on ESC astrocytes. Scale bars in (A) and (B), 50 μ m.

optical stimulation, as well as glial-derived neurotrophic factor (Gdnf), a neurotrophic factor that promotes long-term motor neuron survival (see

supplementary materials and methods). To develop such ESCs suitable for in vivo engraftment of ESC motor neurons, we stably transfected an

established mouse ESC clonal cell line that already carried the motor neuron-specific reporter *Hb9::CD14-IRES-GFP* (GFP, green fluorescent protein) (12) with a photoreceptor transgene that is expressed regardless of cell type, *CAG::ChR2-YFP* (YFP, yellow fluorescent protein), and with the neurotrophin-expressing *CAG::Gdnf* transgene. Embryoid bodies derived from *CAG::ChR2-YFP/Gdnf* ESCs, which express ChR2-YFP in all cells including motor neurons (Fig. 1A), were differentiated in vitro using an established protocol (13, 14). *CAG::ChR2-YFP/Gdnf* motor neurons also produce Gdnf (Fig. 1B), which improves their long-term survival in vitro (Fig. 1C). When cultured on an ESC-derived astrocyte feeder layer (fig. S1), ChR2 motor neurons mature electrically over a period of 35 days, until they fire trains of action potentials in response to optical stimulation and closely resemble adult motor neuron activity patterns induced by electrical stimulation (15) (Fig. 1D and fig. S2).

After developing these ChR2 motor neurons, we next established an in vivo model to assess the feasibility of restoring muscle function with optical control of the engrafted cells, using the sciatic nerve. Muscle denervation was induced by sciatic nerve ligation in adult mice. This procedure results in a complete initial denervation, followed by limited regeneration of endogenous axons through the ligation site, thereby creating a partially denervated environment resembling the partial muscle denervation of early-stage ALS (fig. S3). Three days postligation, embryoid bodies containing ChR2 motor neurons were engrafted distal to the ligation into the tibial and common peroneal branches of the sciatic nerve. Histological analysis revealed that the engrafted ChR2 motor neurons not only survive for at least 35 days in the peripheral nerve environment (Fig. 2A), but also mature morphologically to resemble adult spinal motor neurons and express the mature motor neuron marker choline acetyltransferase (Fig. 2B). Immunodetection of ChR2-YFP, using an antibody to GFP, demonstrates that ChR2 is localized to the membrane of motor neurons, whereas direct detection of GFP versus YFP fluorescent signals reveals that Hb9-driven GFP expression is virtually absent in ChR2 motor neurons that have matured in vivo for 35 days (figs. S4 and S5). Additionally, ChR2 motor neurons extended large numbers of axons (Fig. 2C) distally toward both anterior [tibialis anterior (TA) and extensor digitorum longus (EDL)] and posterior [triceps surae (TS)] lower hind-limb muscles when grafted into the specific branches of the sciatic nerve that innervate these muscles. Engrafted ChR2 motor neuron axons, which grow alongside regenerating endogenous (YFP-negative) motor axons, are mostly myelinated (Fig. 2D). Histological analysis also revealed robust reinnervation of muscle fibers by ChR2 motor neurons, although the neuromuscular junctions exhibited hallmarks of inactivity, including poly-innervation as well as collateral and terminal axonal sprouting (16) (Fig. 2E), most likely because these motor neurons were inactive

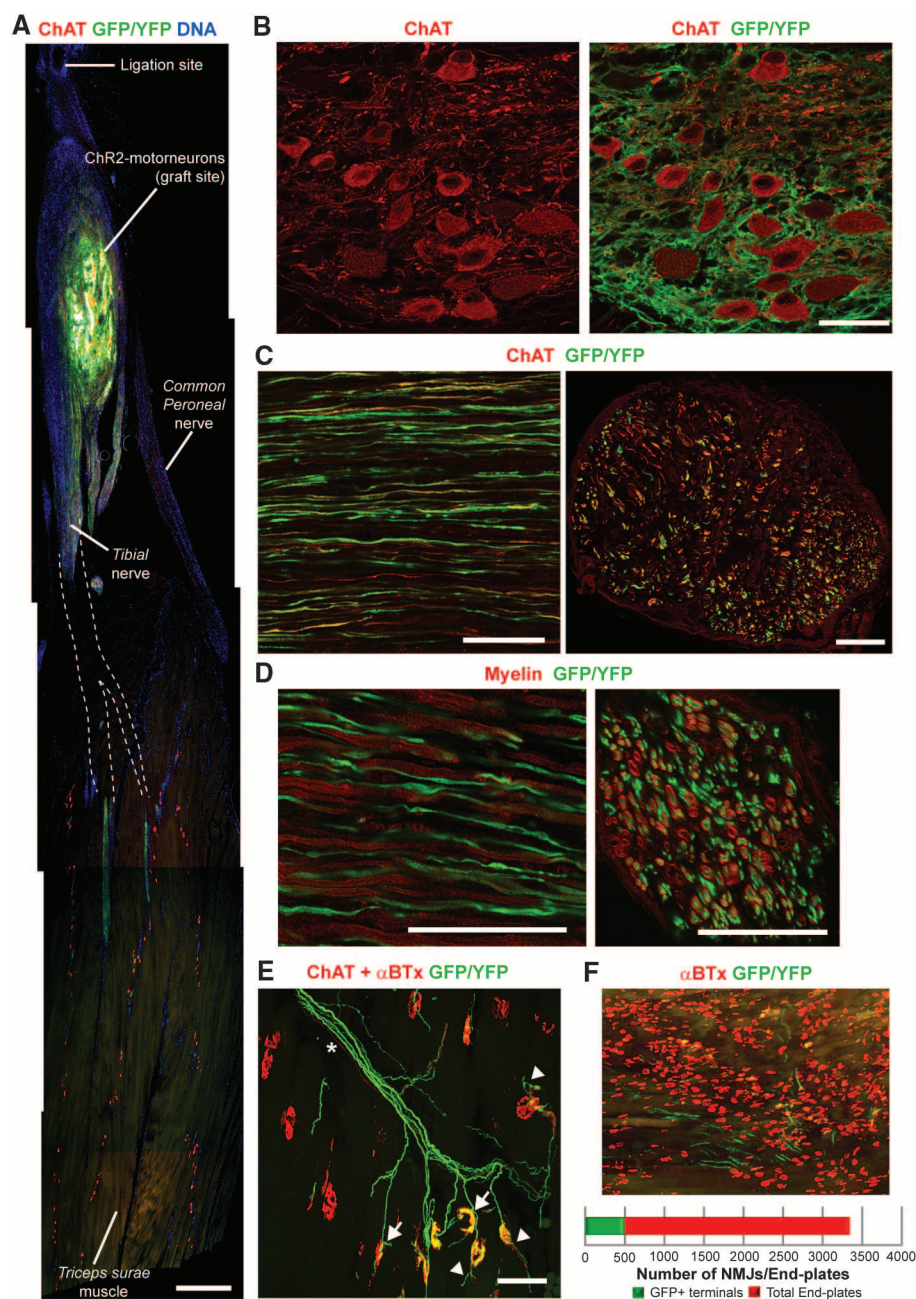


Fig. 2. Robust axonal growth and reinnervation of distal muscles after engraftment of ChR2 motor neurons. (A) Image montage of a whole nerve and muscle section showing ChR2 motor neuron cell bodies at the graft site and axon projection (dashed lines indicate approximate trajectory). Scale bar, 500 μ m. (B) Confocal image of engrafted ChR2 motor neurons immunolabeled for choline acetyltransferase (ChAT; left image) and GFP and/or YFP (merged image at right). Scale bar, 50 μ m. (C) Confocal image of longitudinal and transverse common peroneal nerve sections showing both ChR2 motor neurons and endogenous axons. Scale bar, 50 μ m. (D) Confocal images of engrafted ChR2 motor neuron axons showing myelination. Scale bar, 50 μ m. (E) Confocal z-stack of ChR2 motor neuron axon terminals innervating multiple neuromuscular junctions within the TS muscle. Arrows indicate preterminal collateral sprouting, arrowheads denote terminal sprouting, and the asterisk indicates an endogenous motor axon. Scale bar, 50 μ m. (F) Two-dimensional projection image of a TS muscle showing proportion of neuromuscular junctions (NMJs) innervated by engrafted ChR2 motor neurons, relative to the total number of end plates present [labeled with α -bungarotoxin (α BTx)]. Quantification is shown below. Representative images shown here are compiled from $n = 4$ engrafted nerves from three separate experiments.

in vivo until stimulated by the external optical signal. Nevertheless, quantification of all end plates within a whole TS muscle revealed that 14.7% were innervated by YFP-positive ChR2 motor neurons axons after 35 days (Fig. 2F). Moreover, we observed YFP-positive neuromuscular junctions in both fast-twitch and slow-twitch regions of the TS, indicating that ChR2 motor neurons can innervate different muscle types. Therefore, this time point (35 days) was used in subsequent experiments to establish whether the transplanted ChR2 motor neurons were indeed functional and responsive to optical stimuli in vivo.

In anesthetized animals, we used isometric muscle tension physiology to examine the contractile responses elicited from TA, EDL, and TS (data summarized in table S1) muscles after optical stimulation of the exposed sciatic nerve using finely controlled pulses of 470-nm blue light generated by a light-emitting diode (LED) unit and delivered via a light-guide to the graft site (Fig. 3A and movie S1). Short-duration (14-ms) light pulses were able to induce submaximal twitch contrac-

tions in muscles innervated by transplanted ChR2 motor neurons (Fig. 3B), whereas high-frequency illumination (40 to 80 Hz) induced tetanic muscle contraction (Fig. 3C) that can be repeated in a highly reproducible manner (Fig. 3D). Quantification of these contractile responses demonstrated that the ratio of tetanic to twitch force was 3.09 ± 0.52 and 2.34 ± 0.33 for TA and EDL muscles, respectively (Fig. 3E), similar to normal values in uninjured animals.

Because nerve ligation enables regeneration of some endogenous motor axons, it was possible to directly compare the properties of these endogenous axons with those of the grafted ChR2 motor neurons by electrical nerve stimulation, which activates both populations of axons. This comparison demonstrated that the proportionate increase between twitch and tetanic stimuli after electrical stimulation was similar to that of optical stimulation [3.07 ± 0.5 and 2.96 ± 0.3 for TA and EDL muscles, respectively] (table S1), although maximal force generation induced by optical stimulation of ChR2 motor neurons was weaker in

comparison with electrical recruitment of both ChR2-expressing and endogenous motor neurons (12.2% of electrically induced force for TA and 12.3% for EDL). It is likely that this reduced force output of muscle fibers innervated by ChR2 motor neurons reflects the 35-day period of inactivity preceding optical stimulation, as indicated by the findings of the histological analysis of these muscles, which showed the presence of axonal sprouting and poly-innervated end plates, characteristic features of inactive muscles (16). Sustained optical stimulation in vivo would probably lead to reinforcement of these neuromuscular junctions and a corresponding increase in force output. Analysis of muscle contractile characteristics also revealed that the latency to peak twitch contraction from initiation of the electrical trigger to the LED unit, or direct stimulation of the nerve, was identical for both optical and electrical stimulation (Fig. 3F). This finding indicates that the nerve conduction velocities were similar for both types of stimulation and supports the histological findings showing that axons of ChR2 motor

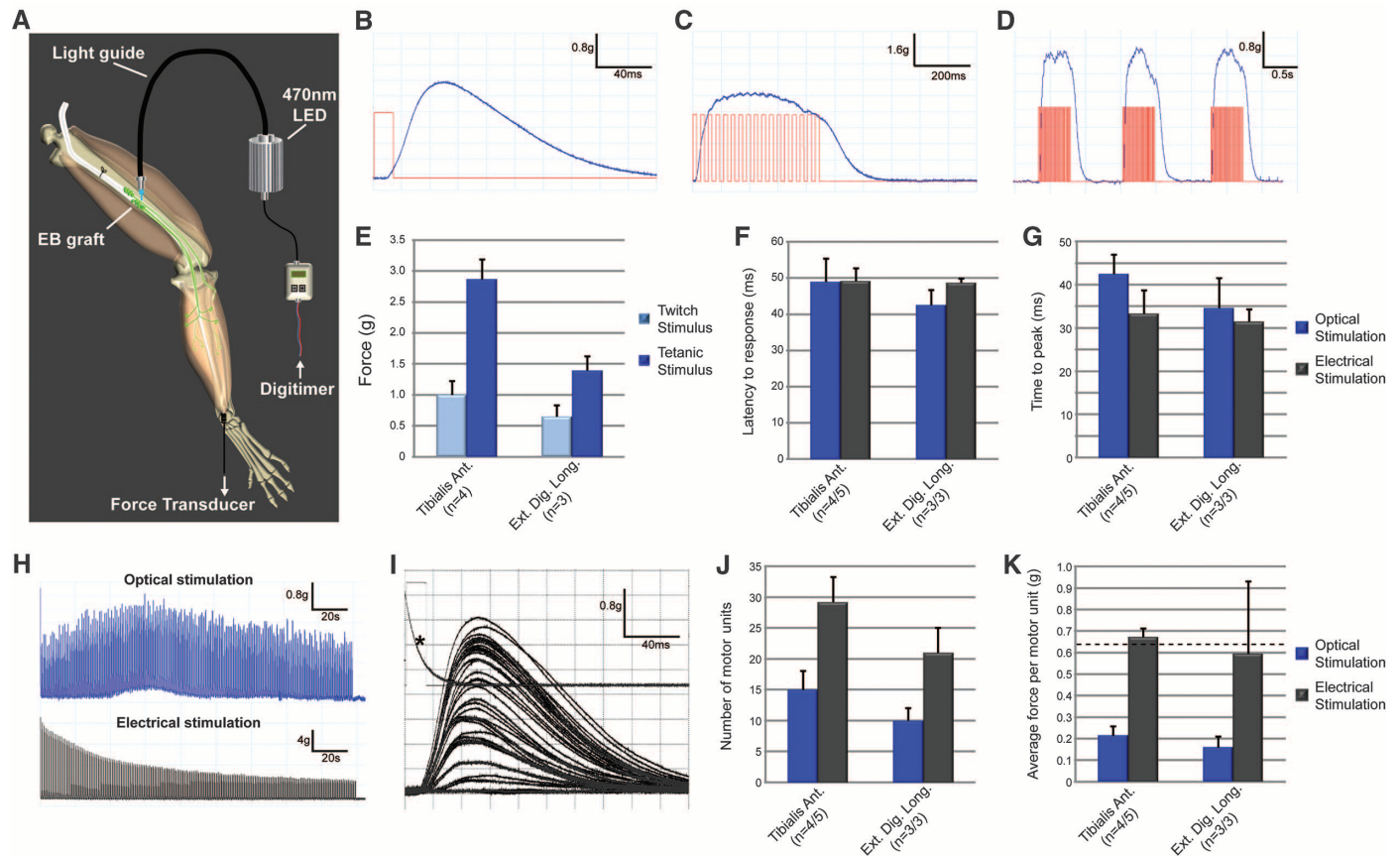


Fig. 3. Restoration of muscle function, in a controlled manner, using optical stimulation of engrafted ChR2 motor neurons in vivo. (A) Schematic showing optical stimulation and isometric muscle tension recordings. EB, embryoid body. Representative twitch (B), tetanic (C), and repetitive tetanic (D) contraction traces obtained from the TA muscle, induced by optical stimulation. Blue line, muscle force; red line, electrical trigger signals sent to the LED unit. (E) Quantification of twitch and tetanic contraction of TA and EDL muscles. Time to peak contractile force, from initiation of the electrical trigger to the LED unit (F) or from the initiation of muscle contraction (G), is shown

alongside direct electrical nerve stimulation (*n* values represent optical/electrical stimulation, respectively, compiled from four separate experiments). (H) Representative fatigue traces from TA muscles (different animals) produced by optical (top) or electrical (bottom) stimulation for 180 s. (I) Representative TA muscle optical stimulation motor-unit number estimate trace. The asterisk indicates square-wave trigger voltage to the LED unit and oscilloscope trigger. (J) Motor-unit number quantification of TA and EDL muscles after optical versus electrical stimulation. (K) Analysis of average motor-unit force. The dashed line indicates the normal EDL value. All error bars indicate SEM.

neurons are myelinated (Fig. 2D). Additionally, the contraction rate—that is, the time from initiation of muscle contraction to peak contraction—was also very similar (Fig. 3G) for both forms of stimulation. Repetitive trains of optical or electrical stimuli (40 Hz, 250-ms duration, every 1 s) were delivered for a period of 180 s to investigate the fatigue characteristics of the reinnervated muscles, which normally have a fast-twitch, fatigable phenotype. The results showed that muscle fibers innervated by grafted Chr2 motor neurons were fatigue-resistant, in contrast to muscle fibers activated by electrical stimulation (Fig. 3H). Again, this probably reflects the prolonged period of inactivity of Chr2 motor neurons before optical stimulation.

Simultaneous activation of all motor neurons innervating a specific muscle would result in inefficient spasmodic contraction and muscle fatigue. It is therefore important that motor neurons are recruited physiologically, according to their activation threshold, to generate a graded muscle contraction that is proportionate to the intended force output. Activation threshold is normally determined by motor neuron soma size (17), but in the case of optogenetic activation of motor neurons, axonal diameter and intermodal distance are also important factors (10, 18). With this in mind, it was important to determine whether grafted Chr2 motor neurons could also be recruited in a graded manner by optical stimulation to induce physiological motor-unit recruitment, where smaller motor units are recruited before larger motor units. To test this, the illumination intensity of the LED was varied from 0.8 to 8 mW/mm², which resulted in stochastic increases in muscle contractile force, demonstrating that different motor units could be recruited according to their optical activation threshold (Fig. 3I). This technique also enabled us to count the number of individual motor units innervating a given muscle, which for the TA muscle was 15 ± 3.03. Furthermore, by comparing optical and electrical nerve stimulation, we found that grafted Chr2 motor neurons accounted for ~50% of all motor units (Fig. 3J). Moreover, the motor-unit counts enabled us to calculate the average motor-unit force (Fig. 3K), which, after optical stimulation, was found to be 0.21 ± 0.04 g and 0.16 ± 0.05 g for TA and EDL muscles, respectively. Combined recruitment of endogenous and Chr2 motor neuron axons by electrical stimulation resulted in average motor-unit force values of 0.67 ± 0.04 g and 0.59 ± 0.34 g for TA and EDL muscles, respectively, consistent with normal motor-unit force (0.62 g).

In this study, we show that Chr2 motor neurons can be successfully transplanted into a peripheral nerve, where they can survive and extend axons that not only replace lost endogenous motor axons but also reinnervate denervated muscle fibers. Moreover, these transplanted Chr2 motor neurons can be selectively activated by 470-nm light, in a controlled manner to produce graded muscle contractions. Major challenges still remain before this approach can be established as an ef-

fective clinical intervention: These obstacles include the development of an implantable optical stimulator, such as that shown by Towne *et al.* (11), and a means to encapsulate the grafted cells. Additionally, incorporation of sensitive, red-shifted channelrhodopsin variants, such as ReaChR (19), rather than Chr2 would abrogate potential cellular toxicity associated with short-wavelength light (20).

These results show that through the use of a synthesis of regenerative medicine and optogenetics, it is possible to restore specific motor nerve functions. Although this study is largely a proof-of-principle study, it is possible that with further development this strategy may be of use in conditions where muscle function is lost—for example, after traumatic injury or neurodegenerative disease.

References and Notes

1. W. W. Glenn, M. L. Phelps, *Neurosurgery* **17**, 974–984 (1985).
2. R. P. Onders *et al.*, *Surg. Endosc.* **23**, 1433–1440 (2009).
3. B. Gernandt, *Acta Physiol. Scand.* **12**, 255–260 (1946).
4. S. C. Zhang, *J. Hematother. Stem Cell Res.* **12**, 625–634 (2003).
5. M. T. Filbin, *Nat. Rev. Neurosci.* **4**, 703–713 (2003).
6. J. M. Harper *et al.*, *Proc. Natl. Acad. Sci. U.S.A.* **101**, 7123–7128 (2004).
7. D. C. Yohn, G. B. Miles, V. F. Rafuse, R. M. Brownstone, *J. Neurosci.* **28**, 12409–12418 (2008).
8. G. Nagel *et al.*, *Proc. Natl. Acad. Sci. U.S.A.* **100**, 13940–13945 (2003).
9. E. S. Boyden, F. Zhang, E. Bamberg, G. Nagel, K. Deisseroth, *Nat. Neurosci.* **8**, 1263–1268 (2005).
10. M. E. Llewellyn, K. R. Thompson, K. Deisseroth, S. L. Delp, *Nat. Med.* **16**, 1161–1165 (2010).
11. C. Towne, K. L. Montgomery, S. M. Iyer, K. Deisseroth, S. L. Delp, *PLoS ONE* **8**, e72691 (2013).
12. C. B. Machado *et al.*, *Development* **141**, 784–794 (2014).

13. H. Wichterle, I. Lieberam, J. A. Porter, T. M. Jessell, *Cell* **110**, 385–397 (2002).
14. M. Peljto, J. S. Dasen, E. O. Mazzoni, T. M. Jessell, H. Wichterle, *Cell Stem Cell* **7**, 355–366 (2010).
15. L. Carrascal, J. L. Nieto-Gonzalez, W. E. Cameron, B. Torres, P. A. Nunez-Abades, *Brain Res. Brain Res. Rev.* **49**, 377–387 (2005).
16. W. J. Thompson, *Cell. Mol. Neurobiol.* **5**, 167–182 (1985).
17. E. Henneman, *Science* **126**, 1345–1347 (1957).
18. J. Tønnesen, *Behav. Brain Res.* **255**, 35–43 (2013).
19. J. Y. Lin, P. M. Knutsen, A. Muller, D. Kleinfeld, R. Y. Tsien, *Nat. Neurosci.* **16**, 1499–1508 (2013).
20. P. E. Hockberger *et al.*, *Proc. Natl. Acad. Sci. U.S.A.* **96**, 6255–6260 (1999).

Acknowledgments: We thank T. Keck, D. Kullman, and G. Schiavo for constructive feedback on the manuscript and the Thierry Latran Foundation for supporting this study. I.L. is funded by the Medical Research Council (G0900585), the Biotechnology and Biological Sciences Research Council (G1001234), King's Health Partners, and the Association Française contre les Myopathies. L.G. is the Graham Watts Senior Research Fellow, funded by The Brain Research Trust, and is supported by the European Community's Seventh Framework Programme (FP7/2007–2013). J.B. is a Wellcome Trust Investigator. The data reported in this paper are tabulated in the supplementary materials. We declare no conflicts of interest. I.L., C.B.M., M.C., and D.S. developed and characterized ESCs, prepared EBs, and purified motor neurons; M.C. and J.B. performed in vitro physiology; J.B.B. performed surgery, in vivo physiology, and histology and drafted the manuscript; V.B.-F. and D.S. assisted with surgery and histology; and L.G. and I.L. developed the original concept, designed and oversaw the study, and revised the manuscript.

Supplementary Materials

www.sciencemag.org/content/344/6179/94/suppl/DC1

Materials and Methods

Figs. S1 to S5

Table S1

References (21–27)

Movie S1

14 November 2013; accepted 5 March 2014

10.1126/science.1248523

Neuronal Control of *Drosophila* Walking Direction

Salil S. Bidaye,* Christian Machacek, Yang Wu,† Barry J. Dickson††

Most land animals normally walk forward but switch to backward walking upon sensing an obstacle or danger in the path ahead. A change in walking direction is likely to be triggered by descending “command” neurons from the brain that act upon local motor circuits to alter the timing of leg muscle activation. Here we identify descending neurons for backward walking in *Drosophila*—the MDN neurons. MDN activity is required for flies to walk backward when they encounter an impassable barrier and is sufficient to trigger backward walking under conditions in which flies would otherwise walk forward. We also identify ascending neurons, MAN, that promote persistent backward walking, possibly by inhibiting forward walking. These findings provide an initial glimpse into the circuits and logic that control walking direction in *Drosophila*.

Walking relies on the intrinsic rhythmic activity of local motor circuits within the central nervous system, called central pattern generators (CPGs). Such locomotor circuits have been documented in a number of species, including cats (1), rodents (2), crayfish (3), stick insects (4), and cockroaches (5). Proprioceptive feedback from leg mechanosensors

ensures the accurate timing of each joint movement, but walking toward or away from specific targets requires descending signals from the brain. These descending inputs might act on CPGs to adjust the order, timing, or amplitude of individual leg movements (6, 7). The nature and identity of these descending commands are poorly understood.